
Multimodal Conditioned Diffusive Time Series Forecasting

Chen Su[♣], Yuanhe Tian[♥], Yan Song^{♣*}

[♣]University of Science and Technology of China

[♥]University of Washington

[♣]suchen4565@mail.ustc.edu.cn [♥]yhtian@uw.edu [♣]clksong@gmail.com

Abstract

Diffusion models achieve remarkable success in processing images and text, and have been extended to special domains such as time series forecasting (TSF). Existing diffusion-based approaches for TSF primarily focus on modeling single-modality numerical sequences, overlooking the rich multimodal information in time series data. To effectively leverage such information for prediction, we propose a multimodal conditioned diffusion model for TSF, namely, MCD-TSF, to jointly utilize timestamps and texts as extra guidance for time series modeling, especially for forecasting. Specifically, Timestamps are combined with time series to establish temporal and semantic correlations among different data points when aggregating information along the temporal dimension. Texts serve as supplementary descriptions of time series' history, and adaptively aligned with data points as well as dynamically controlled in a classifier-free manner. Extensive experiments on real-world benchmark datasets across eight domains demonstrate that the proposed MCD-TSF model achieves state-of-the-art performance.¹

1 Introduction

Time series forecasting (TSF) is a critical task that leverages historical data to predict future time series, enabling proactive decision-making across a wide range of industries. By extracting meaningful insights from temporal dependencies, TSF not only enhances operational efficiency but also mitigates risks, optimizes resource allocation, and supports long-term strategic planning. There are many real-world scenarios TSF has been applied to, such as financial analysis [7, 9, 62], traffic flow estimation [34, 33, 39], climate modeling [58, 66, 67], and energy consumption prediction [37, 22, 8], etc.

With the rise of deep learning, the TSF research shifts from traditional statistical models [4, 11] toward neural networks [41, 5] that exhibit large model capacity, strong scalability, and an end-to-end training paradigm. These models take a time series, i.e., a sequence of values arranged in chronological order, as input and predict values at future times. Specifically, convolutional models [26, 42] leverage kernel and window operations to extract local patterns from time series, whereas they are difficult to obtain the relations among data points at different times. Recurrent models [1, 23] capture temporal dependencies via self-repeating processes, with their deficits in capturing long-distance features. Transformer-based models [30, 13, 68] utilize self-attention mechanisms to model cross dependencies among different data points and generally achieve better performance than the convolutional and recurrent models. In recent years, pretrained models, especially large language models (LLMs), have demonstrated powerful data processing capabilities [2, 17, 51, 60], and TSF datasets are developed with extra annotations (such as timestamps and textual descriptions)

*Corresponding author.

¹The code is available at <https://github.com/synlp/MCD-TSF>.

available along with the time series [28]. Therefore, researchers begin to use LLMs to borrow their knowledge from pretrained data and handle rich inputs of time series such as texts [18, 46, 24]. Straightforwardly, to leverage the LLMs’ inherent capabilities for text-processing, studies [19, 47, 54] generally convert time series directly into text for the model to process, and thus, however, lose the continuous numerical characteristics inherent in time series. Meanwhile, these approaches treat the time series as fixed input, so that slight variations in the input cause significant impact on the prediction results [74, 49]. Consider that a key characteristic of time series data is its presence of a degree of randomness and volatility, such variations should have limited impact on future outcomes. So that the gap between the aforementioned approaches and the characteristics of time series leads to a significant bottleneck and calls for solutions that are able to address this randomness, such as probabilistic models. In doing so, recent studies [38, 50, 27, 15, 43] utilize diffusion networks for TSF. They establish probabilistic relational mappings between historical time series and future data points through parameterized Markov processes. Most of them only use historical time series as input, extracting features from the series itself to condition and guide the diffusion process. Although others [40] generate text descriptions of statistical features (such as the median and trend) of the time series and use these descriptions to enhance the understanding of the time series, they remain restricted by historical time series and textual data, with less attention paid to other types of information, such as timestamps, which encode structural and hierarchical temporal relationships (e.g., day, week, and month) among successive data points, have been demonstrated to provide essential hints for modeling time-related data [53, 65]. Therefore, with the aforementioned limitations from existing studies, it is expected to develop a probabilistic approach to integrate multimodal information, particularly able to process timestamps, thereby enhancing the understanding and forecasting of time series data.

In this paper, we propose a multimodal conditioned diffusion model for TSF, namely, MCD-TSF, which leverages multiple input sources from different modalities such as timestamps and texts to enhance the standard time series input, so as to help the diffusion model to better perform TSF. Specifically, at each diffusion step, we firstly encode the historical time series, timestamps and texts, and then fusing their embeddings, where we integrate timestamp embeddings into time-series embeddings to enhance the understanding for each data point, and then further integrate such enhanced representations with the textual embeddings, so as to progressively guide the denoising process. Moreover, to mitigate the influence of the potentially irrelevant textual content, we employ adaptive balancing technique named classifier-free guidance (CFG) [21] to dynamically fuse the time series representations by two settings: timestamp only or using both timestamp and text, providing better robustness of our approach under variant inputs, e.g., missing the text part. As a result, MCD-TSF allow the TSF task not only leverages the probabilistic nature of diffusion models to accurately capture the inherent randomness of time-series data, but also achieves a deeper and more nuanced understanding of temporal patterns through dynamic fusion of multimodal information. Extensive experiments on multimodal datasets covering eight real-world domains, including transportation, agriculture, weather, economics, and energy, demonstrate the superior generalized performance of our approach, which outperforms strong baselines and existing studies.

2 Related Work

2.1 Diffusion Models for Time Series Modeling

Diffusion models [20, 52, 44] are probabilistic neural approaches widely used for many tasks (e.g., image generation), and have recently been applied to time series modeling [16, 6, 38, 27, 29]. Many diffusion-based studies [50, 14] focus on time series interpolation, where they learn a stochastic mapping from the given time series to the missing values based on their left and right time contexts. These studies conventionally treat historical numerical sequences as denoising conditions to guide the model in reconstructing the time series from Gaussian noise. However, standard diffusion models overlook inherent temporal patterns and multi-scale characteristics in the data, limiting prediction accuracy. To enhance the accuracy of time series prediction, recent studies leverage signal processing techniques such as season-trend decomposition [43], multi-resolution analysis [15, 43], and spectral analysis [63] to extract semantic information from time series data. There are also studies [50, 55] utilizing self-supervised pre-training to learn high-quality representations of time series to improve the understanding of historical time series and thus obtain better TSF performance. Although these approaches provide promising solutions to improving time series modeling, they pay insufficient attention to leveraging extra data or inputs from other modalities that provides important information

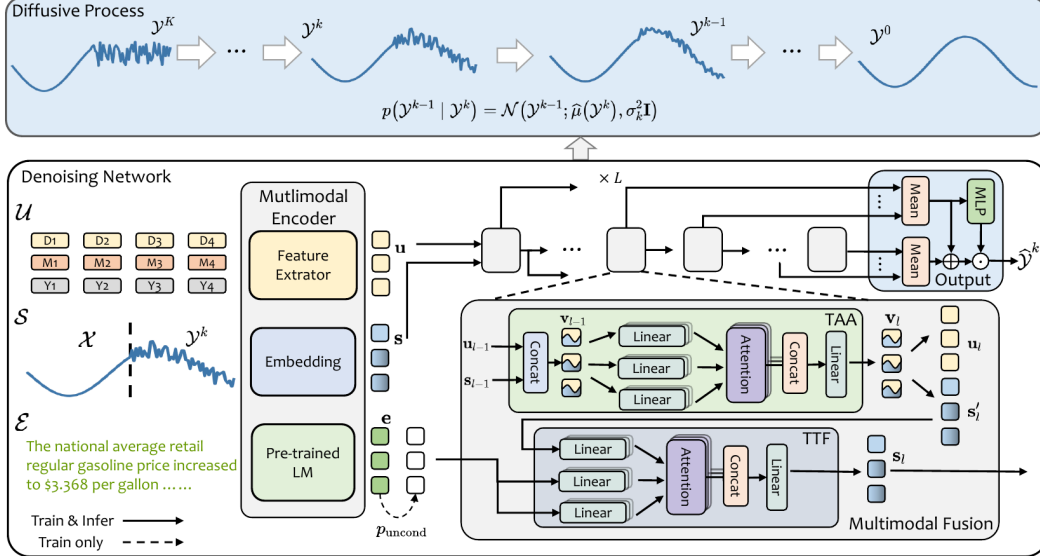


Figure 1: The overall architecture of the proposed MCD-TSF. Our approach consists of four components: the diffusion framework; a multimodal encoder, multimodal fusion module, and an output layer, which are presented at the top, bottom-left, bottom-center, and bottom-right parts of the figure, respectively. The multimodal fusion component internally contains the TAA and TTF modules.

for time series understanding. Meanwhile, existing studies focus on time series interpolation or other time series tasks and, to some extent, merely touch the forecasting task. Compared to existing studies, we apply diffusion models focusing on TSF that predicts the time series based solely on the left context and utilize multimodal inputs such as timestamps and text to facilitate the task.

2.2 Multimodal Time Series Forecasting

Another research line of this work is multimodal TSF, where the models incorporate heterogeneous inputs beyond time series data. Most multimodal studies [35, 64, 69, 57, 71] utilize text as the additional modality to enhance time series inputs. To fuse text information into the time series for TSF, current studies [59, 31, 32, 61] employ LLMs, which are used as backbones and concatenate text embeddings with time series embeddings to form the new input, with the final predicted value sequence generated by mapping the model’s hidden states through linear layers. In doing so, they rely on converting time series into specialized textual data comprehensible to LLMs, thereby losing the numerical information in the original time series data. Some studies [36, 10] directly concatenate time series embeddings with text embeddings as model input and encode them to predict the future values. To further improve model performance, Liu et al. (2024) [28] combine LLM-encoded textual features with single-modal TSF model outputs through learnable linear weighting to produce future values. Zhou et al. (2025) [73] employ cross-attention to enhance cross-modal fusion, subsequently completing predictions via feed-forward networks. Although these approaches achieve fine-grained text-time series fusion, they fail to control the influence of text on time series modeling, leading to textual noise-induced degradation of forecasting accuracy. However, relying on full-scale LLMs for text encoding often incurs excessive compute and memory costs, and is not strictly necessary for TSF tasks where the textual inputs are relatively short and domain-specific. Therefore, there are studies [28] that utilize relatively small pre-trained language models (e.g., BERT [12]) to encode text and fuse the resulting text representations to time series presentations, and obtain promising TSF performance. There are some recent studies [53, 65] that utilize timestamps to enhance TSF, where the timestamps are independently predicted in their models and then combined with the historical time-series-based prediction through weighting to predict the final future values. They focus on integrating global patterns from timestamps while neglecting their roles in representing temporal hierarchical relationships among data points. These approaches are inherently deterministic and therefore cannot quantify the uncertainty in their predictions, nor do they provide a probabilistic view of future trajectories, which is a significant limitation when time series data contain volatility and noise. Compared with existing approaches, our MCD-TSF is designed on diffusion models that

extracts structural temporal cues from timestamps and semantic context from text, then jointly fuses them with the numerical time series to perform uncertainty-aware forecastings.

3 The Approach

The overall architecture of MCD-TSF is illustrated in Figure 1. Given a time series $\mathcal{X} = \{\mathbf{x}_1 \cdots \mathbf{x}_H\}$ of H values (the h -th value is \mathbf{x}_h) with its corresponding timestamps \mathcal{T} and related texts \mathcal{E} , as well as the future timestamps \mathcal{T}' , MCD-TSF progressively predicts the future time series $\mathcal{Y} = \{\mathbf{x}_{H+1} \cdots \mathbf{x}_{H+F}\}$ with F values at future times \mathcal{T}' from a Gaussian noise vector \mathbf{n} through a K -step denoising process $\{\mathcal{Y}^K, \mathcal{Y}^{K-1}, \dots, \mathcal{Y}^k, \mathcal{Y}^{k-1}, \dots, \mathcal{Y}^0\}$, where \mathcal{Y}^k is the denoised output (state) of the diffusion model at the k -th step with the initial \mathcal{Y}^K equaling to \mathbf{n} and the final \mathcal{Y}^0 referring to \mathcal{Y} . The denoising process at each step k is performed by a denoising network f_θ , which takes \mathcal{Y}^k , \mathcal{T}' , and multimodal inputs (including \mathcal{X} , \mathcal{T} , and \mathcal{E}) to predict \mathcal{Y}^{k-1} , where the timestamp and text are used one after the other to enhance the time series representation for better performing the denoising process. By iterating this denoising process K times, we obtain an estimate of the future value $\hat{\mathcal{Y}}$ (which is identical to \mathcal{Y}^0 in the denosing process) in the time series. In the following subsections, we firstly present the principle of diffusive modeling for TSF, then describe the multimodal conditioned diffusive process, and finally illustrate the details of our MCD-TSF model.

3.1 Diffusive Modeling for TSF

Conventional diffusion models consist of a forward noise-addition and a reverse denoising process. In the forward process, the diffusion model iteratively adds Gaussian noise to the target \mathcal{Y} in the sequence of states in the denoising process $\{\mathcal{Y}^k\}_{k=1}^K$. At the k -th diffusion step, the state \mathcal{Y}^k is drawn from the target \mathcal{Y} as follows:

$$p(\mathcal{Y}^k | \mathcal{Y}) = \mathcal{N}(\mathcal{Y}^k; \mu = \sqrt{\bar{\alpha}_k} \mathcal{Y}, \Sigma = (1 - \bar{\alpha}_k) \mathbf{I}) \quad (1)$$

where $p(\cdot | \cdot)$ denotes a conditional probability density function; $\mathcal{N}(x; \mu, \Sigma)$ refers to the multivariate Gaussian distribution with mean vector μ and covariance matrix Σ ; and \mathbf{I} is the identity matrix whose dimensionality matches that of \mathcal{Y} . Herein, $\bar{\alpha}_k = \prod_{i=1}^k \alpha_i$ is the cumulative signal retention factor up to step k , with each $\alpha_i \in (0, 1)$ controlling the proportion of signal preserved (and thus the noise level $1 - \alpha_i$) at step i .

In the reverse process, the diffusion model aims to recover the target \mathcal{Y} from pure noise \mathcal{Y}^K through a parameterized denoising distribution:

$$p(\mathcal{Y}^{k-1} | \mathcal{Y}^k) = \mathcal{N}(\mathcal{Y}^{k-1}; \hat{\mu}(\mathcal{Y}^k), \sigma_k^2 \mathbf{I}) \quad (2)$$

where σ_k^2 is the variance associated with diffusion step k and $\hat{\mu}(\mathcal{Y}^k)$ is computed by

$$\hat{\mu}(\mathcal{Y}^k) = \frac{\sqrt{\bar{\alpha}_k} (1 - \bar{\alpha}_{k-1})}{\sqrt{\bar{\alpha}_{k-1}} (1 - \bar{\alpha}_k)} \mathcal{Y}^k + \frac{\bar{\alpha}_{k-1} - \bar{\alpha}_k}{\sqrt{\bar{\alpha}_{k-1}} (1 - \bar{\alpha}_k)} \hat{\mathcal{Y}}^k \quad (3)$$

where $\hat{\mathcal{Y}}^k$ is obtained through a diffusion network f_θ parameterized by θ via

$$\hat{\mathcal{Y}}^k = f_\theta(\mathcal{Y}^k) \quad (4)$$

By randomly sampling diffusion steps k from a discrete uniform distribution and minimizing the following loss, the parameters θ of the denoising network are learned by

$$\mathcal{L}(\theta) = \mathbb{E}_{k \sim \text{Uniform}\{1, \dots, K\}} \left[\left\| f_\theta(\mathcal{Y}^k) - \mathcal{Y}^* \right\|_2^2 \right] \quad (5)$$

where $\mathcal{L}(\theta)$ is the scalar expected mean squared error loss; $\mathbb{E}[\cdot]$ denotes expectation over the random variable k ; $\text{Uniform}\{1, \dots, K\}$ denotes the discrete uniform distribution on the set $\{1, \dots, K\}$; \mathcal{Y}^* is the gold standard; and $\|\mathbf{v}\|_2 = \sqrt{\sum_{i=1}^d v_i^2}$ is the Euclidean norm of vector $\mathbf{v} \in \mathbb{R}^d$.

When applying the diffusion model on TSF, it utilizes the same forward process as Eq. (1) and conditions the reverse process on historical inputs to help the denoising process. The reverse denoising distribution in Eq. (2) is then formulated as

$$p(\mathcal{Y}^{k-1} | \mathcal{Y}^k, \mathcal{C}) = \mathcal{N}(\mathcal{Y}^{k-1}; \hat{\mu}(\mathcal{Y}^k, \mathcal{C}), \sigma_k^2 \mathbf{I}) \quad (6)$$

where the network f_θ takes \mathcal{Y}^k and condition \mathcal{C} (i.e., the historical inputs), outputs the estimate $\hat{\mu}$ of the next denoised state. Meanwhile, the model still follows Eq. (3) to compute $\hat{\mu}(\mathcal{Y}^k, \mathcal{C})$ with Eq. (4) formulated as

$$\hat{\mathcal{Y}}^k = f_\theta(\mathcal{Y}^k, \mathcal{C}) \quad (7)$$

During training, one minimizes the following conditional loss:

$$\mathcal{L}(\theta) = \mathbb{E}_{k \sim \text{Uniform}\{1, \dots, K\}} \left[\| f_\theta(\mathcal{Y}^k, \mathcal{C}) - \mathcal{Y}^* \|_2^2 \right] \quad (8)$$

so that the diffusion model learns to produce probabilistic forecasts of future values for TSF on the condition \mathcal{C} .

3.2 Multimodal Conditioned Diffusive Process for TSF

With multimodal input, the condition variable \mathcal{C} consists of not only the historical time series \mathcal{X} , but also other sources such as timestamps $\mathcal{U} = [\mathcal{T}, \mathcal{T}']$ (which includes the historical timestamps \mathcal{T} that correspond to \mathcal{X} and the future timestamp \mathcal{T}'), and textual descriptions \mathcal{E} , etc. The forward diffusion process follows the standard procedure in Eq. (1). In the reverse diffusion process, the denoising network uses a conditioned Gaussian distribution to iteratively recover the future time series by

$$p(\mathcal{Y}^{k-1} | \mathcal{Y}^k, \mathcal{X}, \mathcal{U}, \mathcal{E}) = \mathcal{N}(\mathcal{Y}^{k-1}; \hat{\mu}_\theta(\mathcal{Y}^k, \mathcal{X}, \mathcal{U}, \mathcal{E}), \sigma_k^2 I) \quad (9)$$

where $\hat{\mu}_\theta(\mathcal{Y}^k, \mathcal{X}, \mathcal{U}, \mathcal{E})$ is computed by Eq. (3) and Eq. (4) is formulated by

$$\hat{\mathcal{Y}}^k = f_\theta(\mathcal{Y}^k, \mathcal{X}, \mathcal{U}, \mathcal{E}) \quad (10)$$

f_θ is then trained by minimizing the following conditional mean squared error loss

$$\mathcal{L}(\theta) = \mathbb{E}_{k \sim \text{Uniform}\{1, \dots, K\}} \left[\| f_\theta(\mathcal{Y}^k, \mathcal{X}, \mathcal{U}, \mathcal{E}) - \mathcal{Y} \|_2^2 \right] \quad (11)$$

so that the model learns to integrate both timestamp and text information to enhance the timeseries representation for a better denoising process.

As for the text part, since textual information often serves as a coarse-grained supplement for time series data, with its effectiveness easily influenced by text quality across domains, it is necessary to design a special mechanism to control the model’s reliance on textual information during the inference process to balance the enhancement from timestamps or texts. In doing so, CFG, which is experimentally validated in conditional image generation domains and demonstrates its capability to balance specificity and diversity in image generation [21], is utilized to perform our mechanism. In detail, we adjust the prediction $\hat{\mathcal{Y}}$ of the denoising network through a linear combination of text-conditioned and non-text-conditioned (i.e., input text is set to an empty string denoted by \emptyset) components, which is represented by

$$\hat{\mathcal{Y}}_w^k = f_\theta(\mathcal{Y}^k, \mathcal{X}, \mathcal{U}, \emptyset) + w (f_\theta(\mathcal{Y}^k, \mathcal{X}, \mathcal{U}, \mathcal{E}) - f_\theta(\mathcal{Y}^k, \mathcal{X}, \mathcal{U}, \emptyset)) \quad (12)$$

where w is a hyperparameter that controls the model’s reliance on textual information and $\hat{\mathcal{Y}}_w^k$ replace $\hat{\mathcal{Y}}^k$ in Eq. (10) during the diffusion process. In practice, when training the model with and without text conditions (i.e., $f_\theta(\mathcal{Y}^k, \mathcal{X}, \mathcal{U}, \mathcal{E})$ and $f_\theta(\mathcal{Y}^k, \mathcal{X}, \mathcal{U}, \emptyset)$, respectively), we follow [21] to randomly mask the text conditions with a certain probability p_{uncond} , so as to enable simultaneous training of both conditional and unconditional cases for better generalization.

3.3 The MCD-TSF Model

The MCD-TSF consists of three core modules: a multimodal encoder, a stack of Transformer-based fusion layers, and an output layer for adaptive feature fusion.

The multimodal encoder transforms the combined time series $\mathcal{S} = [\mathcal{X}, \mathcal{Y}^k]$, timestamps \mathcal{U} , and text \mathcal{E} into feature embeddings \mathbf{s} , \mathbf{u} , and \mathbf{e} , respectively. Specifically, \mathbf{s} is obtained by applying a 1×1 convolutional layer to extract numerical features from \mathcal{S} . There is a timestamp feature extractor, which firstly disentangles structural attributes (e.g., `DayOfWeek`, `DayOfMonth`, `DayOfYear`) from the raw timestamps, normalizes each to $[-0.5, 0.5]$, which results in vectors such as $[0.166, 0.3, -0.02]$, and then encodes this vector via a 1×1 convolution to produce the embedding \mathbf{u} . The text input \mathcal{E} is

Table 1: Statistics of the dataset. Frequency denotes the temporal recording frequency of the time series; number of samples indicates the quantity of time series samples; text coverage represents the ratio of the number of texts to the number of temporal samples in the domain. ‘‘Arg’’, ‘‘Cli’’, ‘‘Eco’’, ‘‘Ene’’, ‘‘Env’’, ‘‘Hea’’, ‘‘Soc’’, and ‘‘Tra’’ are abbreviations for agriculture, climate, economy, energy, environment, health, social good, and traffic, respectively.

	Agr	Cli	Eco	Ene	Env	Hea	Soc	Tra
Frequency	Monthly	Weekly	Monthly	Weekly	Daily	Weekly	Monthly	Monthly
Number of Samples	496	496	423	1479	11102	1389	900	531
Text Coverage	13.3%	100%	85.4%	37.4%	4.2%	54.9%	41.3%	43.4%

tokenized and encoded using a frozen pretrained language model (e.g., BERT [12]), with its final hidden states serving as the textual embedding \mathbf{e} .

The Transformer-based fusion module contains L layers, where each layer consists of Timestamp-assisted attention (TAA) and text-time series fusion (TTF) to progressively enhance the time-series features.² At layer l , each fusion module takes as input the previous layer’s time-series representation \mathbf{s}_{l-1} , timestamp representation \mathbf{u}_{l-1} , and the static text representation \mathbf{e} , and outputs the timestamp-enhanced sequence representation \mathbf{s}_l , the updated timestamp representation \mathbf{u}_l . Specifically, in TAA, we stack \mathbf{s}_{l-1} and \mathbf{u}_{l-1} to obtain a joint representation $\mathbf{v}_{l-1} = [\mathbf{s}_{l-1}; \lambda \cdot \mathbf{u}_{l-1}]$ (where λ is the weight to control the contribution of the timestamp information). We process \mathbf{v}_{l-1} using a multi-head self-attention and obtain \mathbf{v}_l , which is also formulated as $\mathbf{v}_l = [\mathbf{s}'_l; \mathbf{u}_l]$ with \mathbf{s}'_l and \mathbf{u}_l corresponding to \mathbf{s}_{l-1} and \mathbf{u}_{l-1} , respectively. In TTF, we use text to enhance features in the time series through cross-attention, where the timestamp-enhanced time series features \mathbf{s}'_l serve as queries while the textual features \mathbf{e} act as keys and values. Therefore, we obtain the augmented time series features \mathbf{s}_l that carry the numerical semantics of the time series, temporal structural information from timestamps, and complementary information from textual descriptions. Finally, the computed \mathbf{u}_l and \mathbf{s}_l are fed into the next layer for further processing.

The output layer performs two predictions separately from the layer-wise text-timestamp features $\{\mathbf{s}_l\}_{l=1}^L$ and timestamp features $\{\mathbf{u}_l\}_{l=1}^L$, and then adaptively fuse them to obtain the final output. Specifically, we firstly apply mean pooling to $\{\mathbf{s}_l\}_{l=1}^L$ and $\{\mathbf{u}_l\}_{l=1}^L$ to compute their averaged representations \mathbf{s}_{avg} and \mathbf{u}_{avg} by

$$\mathbf{s}_{\text{avg}} = \frac{1}{\sqrt{L}} \sum_{l=1}^L \mathbf{s}_l, \quad \mathbf{u}_{\text{avg}} = \frac{1}{\sqrt{L}} \sum_{l=1}^L \mathbf{u}_l \quad (13)$$

Then, two multi-layer 1×1 convolutional heads are applied to produce the time series-based and timestamp-based predictions (which are denoted as $(\hat{\mathcal{X}}_s, \hat{\mathcal{Y}}_s)$ and $(\hat{\mathcal{X}}_u, \hat{\mathcal{Y}}_u)$, respectively) by:

$$(\hat{\mathcal{X}}_s, \hat{\mathcal{Y}}_s) = \text{Conv}_s(\mathbf{s}_{\text{avg}}), \quad (\hat{\mathcal{X}}_u, \hat{\mathcal{Y}}_u) = \text{Conv}_u(\mathbf{u}_{\text{avg}}) \quad (14)$$

where $\hat{\mathcal{X}}_s$ and $\hat{\mathcal{Y}}_s$ are the time series-based predictions of the historical time series \mathcal{X} and \mathcal{Y} , respectively; $\hat{\mathcal{X}}_u$ and $\hat{\mathcal{Y}}_u$ are the timestamp-based predictions according to the historical timestamps \mathcal{T} and the future timestamp \mathcal{T}' . Finally, a learnable multi-layer perceptron (MLP) computes fusion weights \mathbf{W} from the differences between $\hat{\mathcal{X}}_u$ and \mathcal{X} by

$$\mathbf{W} = \text{MLP}(\hat{\mathcal{X}}_u - \mathcal{X}) \quad (15)$$

which is used to fuse $\hat{\mathcal{Y}}_s$ and $\hat{\mathcal{Y}}_u$ by

$$\hat{\mathcal{Y}}_{k-1} = \sum \mathbf{W} \odot (\hat{\mathcal{Y}}_s \oplus \hat{\mathcal{Y}}_u) \quad (16)$$

where \odot and \oplus stand for Hadamard product and concatenation operations, respectively, and the resulting $\hat{\mathcal{Y}}^{k-1}$ is fed into the next diffusion step for denoising to \mathcal{Y}^0 .

²The effectiveness of firstly performing TAA and then utilizing TTF is supported by the experimental results in Appendix F.1.

4 Experiment Setting

4.1 Dataset

We follow existing studies [28] to utilize the text-time series benchmark datasets that cover eight domains, namely, *agriculture*, *climate*, *economy*, *energy*, *environment*, *health*, *social good*, and *traffic*, respectively. We normalize the data to regularize it into a distribution with a mean of 0 and a standard deviation of 1. Following existing studies [57, 71], the dataset is then partitioned chronologically into training, validation, and test sets in a 7:1:2 splitting. Table 1 summarizes the key statistics of all domains, including frequency, number of samples, and text coverage.

4.2 Baselines and Comparing Approaches

To evaluate our proposed MCD-TSF, we compare five baseline models illustrated as follows.

- DIFF: the standard diffusion model with time series as the only input.
- DIFF+TAA: it extends the DIFF model by incorporating timestamp input into the time series with the TAA module.
- DIFF+TTF: it extends the DIFF model by adding textual input to the time series through the TTF module.
- DIFF+TAA-T: it builds upon DIFF+TAA with additional textual input and the MM-TSF [28] text integration module. MM-TSF maps the hidden states of the last layer of the LLM into predictions via a linear layer. These predictions are then adaptively weighted and integrated with the forecasting predictions derived from historical time series data.
- DIFF+TTF-T: it enhances DIFF+TTF by including timestamp input and the TimeLinear [65] timestamp integration module. Herein, TimeLinear processes the input timestamps through multiple linear layers and 1×1 convolutional layers, mapping them into predictions, which are then combined with weighted predictions obtained from historical time series.³

To further demonstrate the superiority of MCD-TSF, we also conduct comparisons with a wide range of existing models that are summarized as follows.

- Transformer-based models: Reformer [25], Autoformer [57], FEDformer [71], PatchTST [35], and HCAN (integrated with Informer) [48];
- MLP-based models: FILM [70], DLinear [64], and TimeMixer++ [56];
- State space models: Timemachine [3];
- Probabilistic models: CSDI [50] and D3VAE [27];
- LLM-based models: FPT [72];
- Text-integrated models: TimeLLM [24] and MM-TSF (integrated with Informer) [28];
- Timestamp-integrated models: GLAFF (integrated with DLinear) [53] and TimeLinear [65].

Note that, while CSDI is a self-attention-based diffusion model for TSF that shares similarities with our approach, it solely incorporates temporal sequence inputs and lacks the capability to process multimodal data. GLAFF similarly employs attention to handle temporal-stamp features, but adopts a separate processing paradigm where timestamps and time series are modeled independently when capturing temporal relationships. For all comparing models, we use their official implementations.

4.3 Implementation Details

We pre-process the dataset based on the following configurations. According to [28], the settings of historical time series length and prediction horizon are determined based on the time series frequency. For the time series part, to accommodate them with varying recording frequencies (i.e., monthly, weekly, and daily), we define a historical time series length as 36 months for monthly frequency, 96 weeks for weekly frequency, and 336 days for daily frequency. Meanwhile, the prediction horizon

³Following the convention, our MCD-TSF is equivalent to DIFF+TAA+TTF.

is also frequency-dependent, with three distinct lengths configured for each frequency to more comprehensively evaluate the model’s short-, medium-, and long-term forecasting capabilities. For example, we predict the future values at 6, 12, and 18 months for monthly frequency, at 12, 24, and 48 weeks for weekly frequency series, and at 48, 96, and 192 days for daily frequency series. The configuration of these length settings follows existing TSF studies [57, 71] while incorporating refinements based on the following insights: The minimum forecast length should exceed the temporal granularity of the time series recording interval by at least one hierarchical level to better evaluate model capabilities in capturing long-term dependencies. For instance, with monthly recorded time series (where the recording interval is measured in months), the minimum forecast length should be no less than 6 months. Concurrently, the historical sequence length should be at least twice the forecast length to ensure sufficient historical context supports the predictions. For the timestamp input, their feature dimension aligns with their frequency, e.g., for monthly, weekly, and daily frequencies, the dimensions are set to three, two, and one, respectively.⁴ For the text input, we concatenate all text corresponding to the 36 intervals preceding the end date of the historical time series. For instance, in a daily frequency time series where each interval represents a day, we aggregate texts spanning the 36-day period prior to the series’ end date into a comprehensive final text, which subsequently serves as the associated text for that particular historical time series.⁵

For model architecture, considering pre-trained language models [12, 45] have achieved outstanding performance for text modeling with significantly lower computational cost than LLMs, we employ the pre-trained BERT-base [12] as the text encoder following its default settings, i.e., 12 layers of Transformer with 768-dimensional hidden states. We use 6 multimodal fusion modules, where both TAA and TTF are implemented using the standard multi-head self-attention. The hidden layer dimension of the model is set to 64. For the timestamp weight λ , the default value is set to 1. For the textual guidance strength w , the default value is set to 0.8; and we set the default unconditional training probability p_{uncond} to 0.1. For the diffusion model, we follow the process in Tashiro et al. (2021) [50]⁶ and implement a quadratic noise schedule with an initial noise level of 0.0001. Time steps are set to follow quadratic distribution sampling combined with the denoising diffusion implicit models (DDIM) [44] approach. In training, except for that in BERT-base, all model parameters are updated through the Adam optimizer.

For evaluation, we follow conventional TSF studies [35, 64, 50] to employ mean squared error (MSE) and mean absolute error (MAE) as evaluation metrics, where lower scores mean better performance.⁷ We evaluate the models on the test data of all domains in the benchmark dataset, and report the average performance under short-, medium-, and long-term prediction lengths (e.g., 6, 12, and 18 months for monthly frequency data) correlated with the frequency of each domain. We experiment with various hyperparameter combinations⁸ and select the optimal configuration based on the performance on the validation set. To ensure statistical reliability, all experiments are repeated three times with different random seeds, and final results are the average of the three runs.

5 Results and Analyses

5.1 Overall Results

The comparative results between our approach and different baseline models are shown in Table 2, where the average performance of each model on all datasets is also reported. There are several observations. First, the “DIFF+TAA” and “DIFF+TTF” consistently outperform the standalone “DIFF” model. This improvement is attributed to the enhanced guidance provided by additional timestamps or text inputs during the denoising process, highlighting the importance of multimodal enhancement to conventional TSF modeling. Second, “DIFF+TAA-T” and “DIFF+TTF-T” that utilize both timestamps and text to enhance time series achieve better performance than “DIFF+TAA” and “DIFF+TTF” that only use one of timestamps and text to enhance time series. The results demonstrate that the synergistic fusion of timestamps and textual information yields superior help compared to using either modality independently. Third, the proposed MCD-TSF (equivalent to “DIFF+TAA+TTF”)

⁴The detailed timestamp encoding process is presented in Appendix A.

⁵The details of how we obtain the text are illustrated in Appendix B.

⁶Details of the diffusion step encoding are presented in Appendix C.

⁷We present the details of the evaluation metrics in Appendix D.

⁸Detailed parameter configurations are provided in Appendix E.

Table 2: The (a) MSE and (b) MAE of baselines and MCD-TSF (i.e., DIFF+TAA+TTF). The ‘‘Avg.’’ is the average performance on the test sets of eight domains. The first and second best results (the lower the better) on each domain are marked by **boldface** and underlines, respectively.

(a) MSE Results

	Agr	Cli	Eco	Ene	Env	Hea	Soc	Tra	Avg.
DIFF	0.992	1.794	0.320	0.417	0.339	1.997	1.242	0.133	0.904
DIFF+TAA	0.540	1.717	0.284	0.401	0.284	1.867	1.161	0.102	0.794
DIFF+TAA-T	0.270	<u>1.654</u>	<u>0.281</u>	<u>0.241</u>	<u>0.281</u>	1.860	<u>1.126</u>	0.101	0.726
DIFF+TTF	0.341	1.813	0.411	0.318	0.334	1.837	1.222	0.097	0.796
DIFF+TTF-T	<u>0.259</u>	1.667	0.311	0.305	0.283	<u>1.700</u>	1.147	<u>0.096</u>	<u>0.721</u>
MCD-TSF	0.222	1.583	0.249	0.153	0.275	1.496	1.035	0.093	0.638

(b) MAE Results

	Agr	Cli	Eco	Ene	Env	Hea	Soc	Tra	Avg.
DIFF	0.717	1.325	0.814	0.365	0.424	0.980	0.678	0.213	0.689
DIFF+TAA	0.486	1.301	0.638	0.348	0.382	0.954	<u>0.624</u>	0.174	0.613
DIFF+TAA-T	<u>0.356</u>	<u>1.156</u>	<u>0.423</u>	<u>0.315</u>	<u>0.380</u>	0.994	0.646	<u>0.171</u>	<u>0.554</u>
DIFF+TTF	0.552	1.504	0.448	0.392	0.419	0.944	1.127	0.178	0.695
DIFF+TTF-T	0.381	1.237	0.479	0.350	0.382	<u>0.864</u>	0.654	0.173	0.564
MCD-TSF	0.322	0.971	0.374	0.293	0.379	0.811	0.569	0.159	0.484

consistently outperforms other baselines (i.e., the ‘‘DIFF+TAA-T’’ and ‘‘DIFF+TTF-T’’). This advantage stems from two complementary mechanisms: the TAA module enhances temporal relationship modeling across the entire input time series through timestamp features, while the TTF module performs finer-grained text fusion and controls the strength of text guidance. The two modules enable MCD-TSF to effectively integrate coarse-grained and fine-grained temporal patterns into the time series, resulting in more accurate and robust forecasts across diverse domains.

We further compare our approach with existing studies and present the results⁹ in Table 3, with several observations drawn from it. First, overall, MCD-TSF outperforms all existing models across six model-type categories, which clearly demonstrates its versatile effectiveness. Second, when particularly compared with probabilistic models (i.e., CSDI, D3VAE), MCD-TSF shows lower MSE and MAE on seven out of eight domains. This advantage favors from MCD-TSF’s effective integration of multimodal conditioning, which provides stronger supervision during the denoising process. Third, compared with existing multimodal approaches (including those models that also incorporate textual information or timestamp features as we do), MCD-TSF achieves better performance in on six out of eight domains. This improvement is attributed to that separately encoding timestamps and text and then progressively integrating them with the time series allows the MCD-TSF to fully leverage both modalities to enrich temporal representations and boost forecasting accuracy. In addition, MCD-TSF performs a controlled text fusion, effectively mitigating the influence of textual noise, so that further improves its TSF ability.

5.2 Effect of Timestamp Condition

To explore the effect of the timestamp, we run different configurations of the timestamp weight λ to control the contribution of timestamp information to enhancing the time series representation, and perform a case study to visualize the effect of timestamps on model performance.

For the effect of λ , we try different values, including 0.2, 0.4, 0.6, 0.8, and 1.0, and report the results on *agriculture*, *economy*, *social good*, and *traffic* domains in Figure 2.¹⁰ Herein, higher λ refers to a higher contribution of the timestamp in the fusion process of the time series. The results show that

⁹For each domain, Table 3 reports the average model performance under different configurations specified in Section 4.3, where the full result on each configuration is reported in Appendix F.2.

¹⁰The results on the other four domains are reported in Appendix F.3.

Table 3: Performance (MSE and MAE) comparison between our approach and existing studies, which are categorized into several groups based on their model types.

(a) MSE Results

	Agr	Cli	Eco	Ene	Env	Hea	Soc	Tra	Avg.
Reformer	2.228	1.334	0.805	0.491	0.320	1.730	1.410	0.346	1.083
Autoformer	0.504	1.948	0.305	0.413	0.377	<u>1.434</u>	1.287	0.159	0.803
FEDformer	0.603	2.396	0.290	0.410	0.303	1.598	1.526	0.159	0.910
PatchTST	0.386	1.580	0.293	0.220	0.254	1.557	1.066	0.124	0.685
HCAN	0.460	1.253	0.379	0.464	0.287	1.883	<u>1.038</u>	0.254	0.752
FiLM	0.675	2.728	0.437	0.354	0.285	2.009	1.834	0.158	1.060
DLinear	1.581	0.950	1.278	0.311	0.283	1.554	1.415	0.281	0.956
TimeMixer++	0.336	1.380	0.330	0.229	0.290	1.866	1.173	<u>0.101</u>	0.713
Timemachine	<u>0.304</u>	1.797	0.281	0.264	0.276	1.666	1.341	0.102	0.753
CSDI	2.096	1.264	1.492	0.410	0.291	1.685	1.112	0.115	1.058
D3VAE	1.166	<u>1.220</u>	0.661	0.286	0.755	1.815	1.098	0.232	0.904
FPT	0.448	1.775	0.303	0.234	0.283	1.551	1.047	0.182	0.727
TimeLLM	0.425	1.417	<u>0.276</u>	<u>0.203</u>	0.277	1.519	1.155	0.141	<u>0.676</u>
MM-TSF	0.714	1.278	1.103	0.610	0.336	1.368	1.067	0.225	0.837
GLAFF	0.432	2.021	0.391	0.217	0.283	1.563	1.039	0.112	0.757
TimeLinear	0.497	1.723	0.327	0.261	0.284	1.556	1.518	0.163	0.791
MCD-TSF (ours)	0.222	1.583	0.249	0.153	<u>0.275</u>	1.496	1.035	0.093	0.638

(b) MAE Results

	Agr	Cli	Eco	Ene	Env	Hea	Soc	Tra	Avg.
Reformer	1.150	1.094	0.745	0.531	0.448	0.860	0.848	0.499	0.771
Autoformer	0.538	1.394	0.439	0.454	0.438	0.895	0.725	0.270	0.644
FEDformer	0.628	1.674	0.424	0.458	0.412	0.943	0.926	0.291	0.719
PatchTST	0.404	1.240	0.408	<u>0.307</u>	0.367	0.863	0.576	0.229	0.549
HCAN	0.552	0.955	0.465	0.452	0.420	0.869	0.587	0.402	0.587
FiLM	0.577	1.870	0.540	0.426	0.388	1.143	1.046	0.292	0.785
DLinear	0.997	0.840	0.932	0.380	0.382	0.878	0.848	0.401	0.707
TimeMixer++	0.400	<u>0.909</u>	0.430	0.337	0.448	0.933	0.589	<u>0.169</u>	<u>0.526</u>
Timemachine	<u>0.358</u>	1.046	0.408	0.373	0.381	0.878	0.606	0.174	0.528
CSDI	1.048	1.028	0.968	0.433	0.391	0.857	<u>0.573</u>	0.238	0.692
D3VAE	0.822	1.024	0.612	0.387	0.730	0.893	0.632	0.367	0.683
FPT	0.510	1.057	0.437	0.362	0.406	0.844	0.587	0.317	0.565
TimeLLM	0.491	0.921	<u>0.397</u>	0.336	0.398	0.818	0.631	0.227	0.527
MM-TSF	0.607	1.041	0.820	0.601	0.467	0.760	0.598	0.402	0.662
GLAFF	0.553	1.208	0.499	0.326	0.398	0.848	0.576	0.206	0.576
TimeLinear	0.549	1.034	0.457	0.389	0.387	0.851	0.884	0.300	0.606
MCD-TSF (ours)	0.322	0.971	0.374	0.293	<u>0.379</u>	<u>0.811</u>	0.569	0.159	0.484

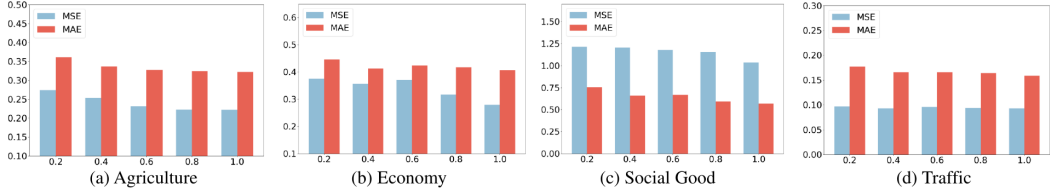


Figure 2: Results of our approach on different domains when configured with various values of the timestamp weights (i.e., the $\lambda = 0.2, 0.4, 0.6, 0.8, 1.0$).

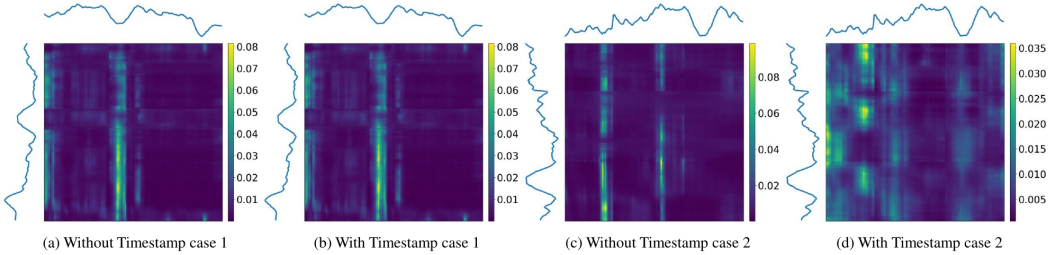


Figure 3: Visual of the attention of our approach across data points of two cases with different settings, where darker colors refer to higher attention weights. Figures (a) and (c) are the attentions from models without using timestamps for case 1 and case 2, respectively; and Figures (b) and (d) are the attentions from models with timestamps for case 1 and case 2, respectively.

our approach achieves better performance across all domains with higher values of λ , which confirms the effectiveness of leveraging timestamp information for TSF.

To further analyze the importance of timestamp fusion for time series modeling, we present the attention heatmaps of two cases from the fourth layer of the TAA module during MCD-TSF’s prediction process with and without the timestamp input on the *Energy* domain dataset in Figure 3, where brighter colors stand for higher attention weights. There are following observations. First, we observe that both models with and without timestamps present brighter colors at the peaks and troughs of the time series, indicating their capability to focus on numerically critical segments (i.e., local maxima and minima). Second, the timestamp-enhanced model displays equally bright colors in additional segments of the time series, accompanied by intricate attention patterns. This demonstrates that the TAA module is able to effectively enhance the model’s attention to temporally relevant features and thus improve the representations of the time series for TSF.

5.3 Effect of Text Condition

To investigate the effect of text modality on TSF, we analyze the effect of two hyperparameters, namely, the textual guidance strength w used only in inference to control the contribution of text to TSF, and the unconditional training probability p_{uncond} employed only in training to influence how much text information is learned to guide TSF. The following are the details.

For textual guidance strength w , we adjust its value within the range $[0.1, 2.5]$ (specifically, we try the values of 0.1, 0.2, 0.3, 0.4, 0.5, 0.6, 0.7, 0.8, 0.9, 1.0, 1.5, 2.0, and 2.5), and analyze performance variations across different domains. We present the curve of MSE variation¹¹ on the test sets of eight domains with respect to the value of w in Figure 4(a). There are following observations. First, overall, on most domains (e.g., the *economy*), the MSE initially decreases and then subsequently increases as the value of guidance strength grows, indicating diminished model performance under both insufficient and excessive textual guidance. The following are the explanations. An insufficient w fails to effectively leverage textual information for prediction guidance, while an overly large w over-prioritizes textual inputs at the expense of historical time series patterns and temporal information. Second, there are domains where the fluctuation of the curve is not significant (e.g., the *environment*

¹¹The MSE variation for a domain is calculated by subtracting the domain’s mean MSE from the obtained MSEs under different guidance strength w , thereby enabling a more intuitive comparison of the trends in model performance across different domains.

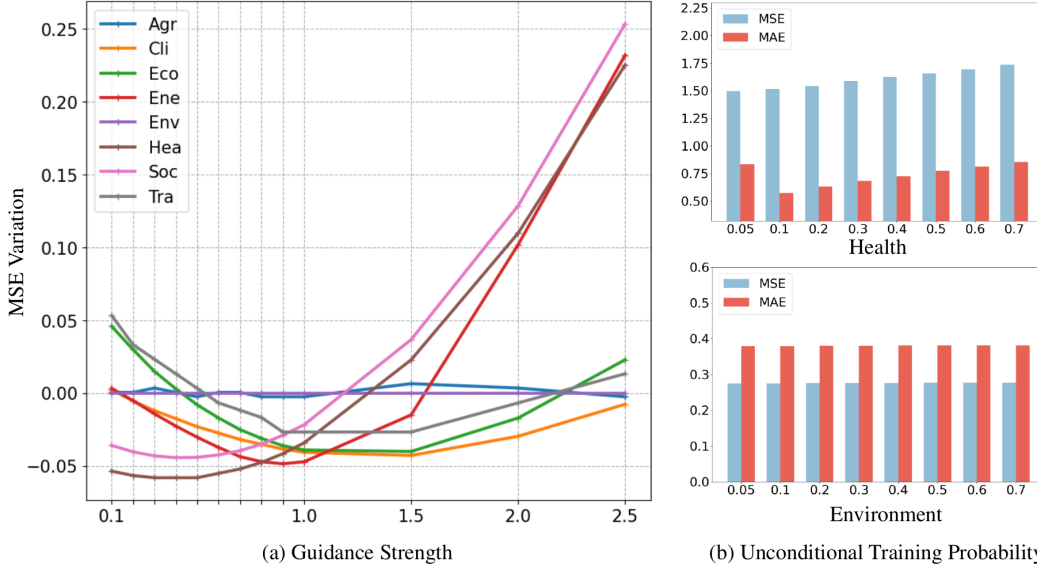


Figure 4: Figure (a) illustrates how the model’s MSE varies with different guidance strengths across datasets from multiple domains, where the reported MSE for each configuration is calculated by subtracting the mean MSE across all configurations within the respective domain. Figure (b) displays the model performance with changes in the unconditional training probability.

domain), which is potentially due to the extreme sparsity of textual data in the domain data. Third, most domains present relatively flat error curves near their minima, indicating the robustness of the proposed model in leveraging text information to enhance the representation of time series.

For unconditional training probability p_{uncond} , we try the following values: 0.05, 0.1, 0.2, 0.3, 0.4, 0.5, 0.6, and 0.7. Figure 4(b) presents two representative results¹² from *health* and *environment* domains. For the results on the *health* domain, the MSE and MAE increase with higher p_{uncond} . This observation is intuitive since a higher p_{uncond} indicates more textual information is masked during training, which prevents the model from effectively leveraging the textual information to enhance the time series representations and thus leads to inferior performance. For the results on the *environment* domain, the change in model performance is not noticeable, which aligns with the results presented in 4(a) and is attributed to the extreme sparsity of textual data in this domain.

5.4 Case Study

To qualitatively evaluate the advantages of TSF with multimodal input, Figure 5 presents several prediction results from two baselines (i.e., PatchTST [35], and CSDI [50]) and MCD-TSF in the *energy* domain from the experiment dataset. The selected cases illustrate non-stationary time series where accurate forecasting requires models to comprehensively understand dynamic variations rather than merely replicating historical patterns. Observations reveal that all baselines and our approach produce prediction curves closely aligned with the ground truth for short-term forecasting. However, in extending forecasting horizons, the curves from both PatchTST and CSDI show significant deviations from the ground truth. Particularly, CSDI captures general trend similarities with the ground truth but fails to predict inflections in the forecast horizon, which suggests that although, to some extent, CSDI learns the relations among different timestamps, it still lacks robustness for longer-term predictions. PatchTST predicts variations in the time series that closely resemble the patterns in historical time series, highlighting that the model heavily relies on past data. In contrast, MCD-TSF accurately captures the complete temporal evolution throughout the forecast period, maintaining close alignment with the Ground Truth. This indicates that MCD-TSF effectively learns the intrinsic dynamics of time series through multimodal assistance of temporal and textual information.

¹²The results on the other domains are reported in Appendix F.4.

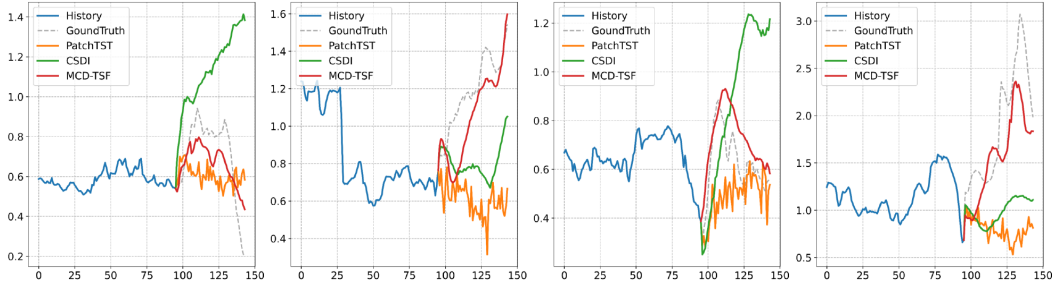


Figure 5: Case study with four examples from *energy* domains. In all cases, the historical time series and the gold standard future time series are marked by blue and dashed grey lines, respectively. The predictions from PatchTST, CSDI, and our approach (i.e., MCD-TSF) are represented by orange, green, and red lines, respectively.

6 Conclusion

In this paper, we propose a novel multimodal diffusion model for TSF, named MCD-TSF, which incorporates extra two modalities, e.g., timestamps and text, to model the temporal relationships among data points and enrich the semantic information of the time series. Specifically, upon a Transformer-based diffusion implementation, a multimodal fusion module with TAA and TTF is proposed to incorporate the aforementioned multimodal inputs, thereby progressively enhancing the representations of time series data. Classifier-free guidance (CFG) is utilized to further dynamically control the impact of the text information on the enhanced time series representations. Extensive experiment results and analyses on real-world datasets across eight domains show that MCD-TSF achieves better predictions compared to strong baselines and existing studies for TSF.

References

- [1] Hossein Abbasimehr and Reza Paki. Improving Time Series Forecasting Using LSTM and Attention Models. *Journal of Ambient Intelligence and Humanized Computing*, 13(1):673–691, 2022.
- [2] Josh Achiam, Steven Adler, Sandhini Agarwal, Lama Ahmad, Ilge Akkaya, Florencia Leoni Aleman, Diogo Almeida, Janko Altenschmidt, Sam Altman, Shyamal Anadkat, et al. GPT-4 Technical Report. *arXiv preprint arXiv:2303.08774*, 2023.
- [3] Md Atik Ahamed and Qiang Cheng. TimeMachine: A Time Series Is Worth 4 Mambas for Long-Term Forecasting. In *27th European Conference on Artificial Intelligence*, volume 392, page 1688, 2024.
- [4] Adebisi A Ariyo, Adewumi O Adewumi, and Charles K Ayo. Stock Price Prediction Using the ARIMA Model. In *2014 UKSim-AMSS 16th International Conference on Computer Modelling and Simulation*, pages 106–112. IEEE, 2014.
- [5] Anastasia Borovykh, Sander Bohte, and Cornelis W Oosterlee. Conditional Time Series Forecasting With Convolutional Neural Networks. *arXiv preprint arXiv:1703.04691*, 2017.
- [6] Borui Cai, Shuiqiao Yang, Longxiang Gao, and Yong Xiang. Hybrid Variational Autoencoder for Time Series Forecasting. *Knowledge-Based Systems*, 281:111079, 2023.
- [7] Jian Cao, Zhi Li, and Jian Li. Financial Time Series Forecasting Model Based on CEEMDAN and LSTM. *Physica A: Statistical Mechanics and Its Applications*, 519:127–139, 2019.
- [8] VS Chandrika, NMG Kumar, Vinjamuri Venkata Kamesh, A Shobanadevi, V Maheswari, K Sekar, T Logeswaran, and A Rajaram. Advanced LSTM-Based Time Series Forecasting for Enhanced Energy Consumption Management in Electric Power Systems. *International Journal of Renewable Energy Research (IJRER)*, 14(1):127–139, 2024.
- [9] Dawei Cheng, Fangzhou Yang, Sheng Xiang, and Jin Liu. Financial Time Series Forecasting With Multi-Modality Graph Neural Network. *Pattern Recognition*, 121:108218, 2022.

- [10] Yu-Neng Chuang, Songchen Li, Jiayi Yuan, Guanchu Wang, Kwei-Herng Lai, Leisheng Yu, Sirui Ding, Chia-Yuan Chang, Qiaoyu Tan, Daochen Zha, et al. Understanding Different Design Choices in Training Large Time Series Models. *arXiv preprint arXiv:2406.14045*, 2024.
- [11] Javier Contreras, Rosario Espinola, Francisco J Nogales, and Antonio J Conejo. ARIMA Models to Predict Next-Day Electricity Prices. *IEEE Transactions on Power Systems*, 18(3):1014–1020, 2003.
- [12] Jacob Devlin, Ming-Wei Chang, Kenton Lee, and Kristina Toutanova. Bert: Pre-training of Deep Bidirectional Transformers for Language Understanding. In *Proceedings of the 2019 conference of the North American chapter of the association for computational linguistics: human language technologies, volume 1 (long and short papers)*, pages 4171–4186, 2019.
- [13] Dazhao Du, Bing Su, and Zhewei Wei. Preformer: Predictive Transformer With Multi-Scale Segment-Wise Correlations for Long-Term Time Series Forecasting. In *ICASSP 2023-2023 IEEE International Conference on Acoustics, Speech and Signal Processing (ICASSP)*, pages 1–5. IEEE, 2023.
- [14] Jinxiao Fan, Mengshi Qi, Liang Liu, and Huadong Ma. Diffusion-Driven Incomplete Multimodal Learning for Air Quality Prediction. *ACM Transactions on Internet of Things*, 6(1):1–24, 2025.
- [15] Xinyao Fan, Yueying Wu, Chang Xu, Yuhao Huang, Weiqing Liu, and Jiang Bian. MG-TSD: Multi-granularity Time Series Diffusion Models with Guided Learning Process. *arXiv preprint arXiv:2403.05751*, 2024.
- [16] Shibo Feng, Chunyan Miao, Ke Xu, Jiaxiang Wu, Pengcheng Wu, Yang Zhang, and Peilin Zhao. Multi-Scale Attention Flow for Probabilistic Time Series Forecasting. *IEEE Transactions on Knowledge and Data Engineering*, 36(5):2056–2068, 2023.
- [17] Aaron Grattafiori, Abhimanyu Dubey, Abhinav Jauhri, Abhinav Pandey, Abhishek Kadian, Ahmad Al-Dahle, Aiesha Letman, Akhil Mathur, Alan Schelten, Alex Vaughan, et al. The LLaMA 3 Herd of Models. *arXiv preprint arXiv:2407.21783*, 2024.
- [18] Nate Gruver, Marc Finzi, Shikai Qiu, and Andrew G Wilson. Large Language Models Are Zero-Shot Time Series Forecasters. *Advances in Neural Information Processing Systems*, 36:19622–19635, 2023.
- [19] Nate Gruver, Marc Finzi, Shikai Qiu, and Andrew G Wilson. Large Language Models Are Zero-Shot Time Series Forecasters. *Advances in Neural Information Processing Systems*, 36:19622–19635, 2023.
- [20] Jonathan Ho, Ajay Jain, and Pieter Abbeel. Denoising Diffusion Probabilistic Models. In *Neural Information Processing Systems*, volume 33, pages 6840–6851, 2020.
- [21] Jonathan Ho and Tim Salimans. Classifier-free diffusion guidance. *arXiv preprint arXiv:2207.12598*, 2022.
- [22] Yuqing Hu, Xiaoyuan Cheng, Suhang Wang, Jianli Chen, Tianxiang Zhao, and Enyan Dai. Times Series Forecasting for Urban Building Energy Consumption Based on Graph Convolutional Network. *Applied Energy*, 307:118231, 2022.
- [23] Yuxin Jia, Youfang Lin, Xinyan Hao, Yan Lin, Shengnan Guo, and Huaiyu Wan. WITran: Water-Wave Information Transmission and Recurrent Acceleration Network for Long-Range Time Series Forecasting. *Advances in Neural Information Processing Systems*, 36:12389–12356, 2023.
- [24] Ming Jin, Shiyu Wang, Lintao Ma, Zhixuan Chu, James Y Zhang, Xiaoming Shi, Pin-Yu Chen, Yuxuan Liang, Yuan-Fang Li, Shirui Pan, et al. Time-LLM: Time Series Forecasting by Reprogramming Large Language Models. *arXiv preprint arXiv:2310.01728*, 2023.
- [25] Nikita Kitaev, Łukasz Kaiser, and Anselm Levskaya. Reformer: The Efficient Transformer. *arXiv preprint arXiv:2001.04451*, 2020.
- [26] Zhichen Lai, Dalin Zhang, Huan Li, Christian S Jensen, Hua Lu, and Yan Zhao. LightCTS: A Lightweight Framework for Correlated Time Series Forecasting. *Proceedings of the ACM on Management of Data*, 1(2):1–26, 2023.
- [27] Yan Li, Xinjiang Lu, Yaqing Wang, and Dejing Dou. Generative Time Series Forecasting with Diffusion, Denoise, and Disentanglement. In *Neural Information Processing Systems*, volume 35, pages 23009–23022, 2022.

- [28] Haoxin Liu, Shangqing Xu, Zhiyuan Zhao, Lingkai Kong, Harshvardhan Prabhakar Kamarthi, Aditya Sasanur, Megha Sharma, Jiaming Cui, Qingsong Wen, Chao Zhang, et al. Time-MMD: Multi-Domain Multimodal Dataset for Time Series Analysis. *Advances in Neural Information Processing Systems*, 37:77888–77933, 2024.
- [29] Jingwei Liu, Ling Yang, Hongyan Li, and Shenda Hong. Retrieval-Augmented Diffusion Models for Time Series Forecasting. *Advances in Neural Information Processing Systems*, 37:2766–2786, 2024.
- [30] Shizhan Liu, Hang Yu, Cong Liao, Jianguo Li, Weiyao Lin, Alex X Liu, and Schahram Dustdar. Pyraformer: Low-Complexity Pyramidal Attention for Long-Range Time Series Modeling and Forecasting. In *International Conference on Learning Representations*, 2022.
- [31] Xu Liu, Junfeng Hu, Yuan Li, Shizhe Diao, Yuxuan Liang, Bryan Hooi, and Roger Zimmermann. Unitime: A Language-Empowered Unified Model for Cross-Domain Time Series Forecasting. In *Proceedings of the ACM Web Conference 2024*, pages 4095–4106, 2024.
- [32] Yong Liu, Guo Qin, Xiangdong Huang, Jianmin Wang, and Mingsheng Long. AutoTimes: Autoregressive Time Series Forecasters via Large Language Models. *Advances in Neural Information Processing Systems*, 37:122154–122184, 2024.
- [33] Changxi Ma, Guowen Dai, and Jibiao Zhou. Short-Term Traffic Flow Prediction for Urban Road Sections Based on Time Series Analysis and LSTM-BiLSTM Method. *IEEE Transactions on Intelligent Transportation Systems*, 23(6):5615–5624, 2021.
- [34] Changxi Ma, Guowen Dai, and Jibiao Zhou. Short-Term Traffic Flow Prediction for Urban Road Sections Based on Time Series Analysis and LSTM_BiLSTM Method. *IEEE Transactions on Intelligent Transportation Systems*, 23(6):5615–5624, 2021.
- [35] Yuqi Nie, Nam H Nguyen, Phanwadee Sinthong, and Jayant Kalagnanam. A Time Series Is Worth 64 Words: Long-Term Forecasting with Transformers. *arXiv preprint arXiv:2211.14730*, 2022.
- [36] Zijie Pan, Yushan Jiang, Sahil Garg, Anderson Schneider, Yuriy Nevmyvaka, and Dongjin Song. S²IP-LLM: Semantic Space Informed Prompt Learning With LLM for Time Series Forecasting. In *Forty-First International Conference on Machine Learning*, 2024.
- [37] Tiago Pinto, Isabel Praça, Zita Vale, and Jose Silva. Ensemble Learning for Electricity Consumption Forecasting in Office Buildings. *Neurocomputing*, 423:747–755, 2021.
- [38] Kashif Rasul, Calvin Seward, Ingmar Schuster, and Roland Vollgraf. Autoregressive Denoising Diffusion Models for Multivariate Probabilistic Time Series Forecasting. In *International Conference on Machine Learning*, pages 8857–8868. PMLR, 2021.
- [39] Selim Reza, Marta Campos Ferreira, José JM Machado, and João Manuel RS Tavares. A Multi-Head Attention-Based Transformer Model for Traffic Flow Forecasting With a Comparative Analysis to Recurrent Neural Networks. *Expert Systems with Applications*, 202:117275, 2022.
- [40] Weilin Ruan, Siru Zhong, Haomin Wen, and Yuxuan Liang. Vision-Enhanced Time Series Forecasting via Latent Diffusion Models. *arXiv preprint arXiv:2502.14887*, 2025.
- [41] Alaa Sagheer and Mostafa Kotb. Time Series Forecasting of Petroleum Production Using Deep LSTM Recurrent Networks. *Neurocomputing*, 323:203–213, 2019.
- [42] Li Shen, Yuning Wei, Yangzhu Wang, and Huaxin Qiu. FDNet: Focal Decomposed Network for Efficient, Robust and Practical Time Series Forecasting. *Knowledge-Based Systems*, 275:110666, 2023.
- [43] Lifeng Shen, Weiyu Chen, and James Kwok. Multi-Resolution Diffusion Models for Time Series Forecasting. In *International Conference on Learning Representations*, 2024.
- [44] Jiaming Song, Chenlin Meng, and Stefano Ermon. Denoising Diffusion Implicit Models. *arXiv preprint arXiv:2010.02502*, 2020.
- [45] Yan Song, Tong Zhang, Yonggang Wang, and Kai-Fu Lee. Zen 2.0: Continue Training and Adaption for N-gram Enhanced Text Encoders. *arXiv preprint arXiv:2105.01279*, 2021.
- [46] Chenxi Sun, Hongyan Li, Yaliang Li, and Shenda Hong. TEST: Text Prototype Aligned Embedding to Activate LLM’s Ability for Time Series. *arXiv preprint arXiv:2308.08241*, 2023.
- [47] Chenxi Sun, Hongyan Li, Yaliang Li, and Shenda Hong. TEST: Text Prototype Aligned Embedding to Activate LLM’s Ability for Time Series. *arXiv preprint arXiv:2308.08241*, 2023.

- [48] Yanru Sun, Zongxia Xie, Dongyue Chen, Emadeldeen Eldele, and Qinghua Hu. Hierarchical Classification Auxiliary Network for Time Series Forecasting. *arXiv preprint arXiv:2405.18975*, 2024.
- [49] Hua Tang, Chong Zhang, Mingyu Jin, Qinkai Yu, Zhenting Wang, Xiaobo Jin, Yongfeng Zhang, and Mengnan Du. Time Series Forecasting With LLMs: Understanding and Enhancing Model Capabilities. *ACM SIGKDD Explorations Newsletter*, 26(2):109–118, 2025.
- [50] Yusuke Tashiro, Jiaming Song, Yang Song, and Stefano Ermon. CSDI: Conditional Score-Based Diffusion Models for Probabilistic Time Series Imputation. In *Neural Information Processing Systems*, volume 34, pages 24804–24816, 2021.
- [51] Yuanhe Tian, Ruyi Gan, Yan Song, Jiaying Zhang, and Yongdong Zhang. Chimed-GPT: A Chinese Medical Large Language Model With Full Training Regime and Better Alignment to Human Preferences. *arXiv preprint arXiv:2311.06025*, 2023.
- [52] Yuanhe Tian, Fei Xia, and Yan Song. Diffusion Networks with Task-Specific Noise Control for Radiology Report Generation. In *Proceedings of the 32nd ACM International Conference on Multimedia*, pages 1771–1780, 2024.
- [53] Chengsen Wang, Qi Qi, Jingyu Wang, Haifeng Sun, Zirui Zhuang, Jinming Wu, and Jianxin Liao. Rethinking the Power of Timestamps for Robust Time Series Forecasting: A Global-Local Fusion Perspective. *arXiv preprint arXiv:2409.18696*, 2024.
- [54] Chengsen Wang, Qi Qi, Jingyu Wang, Haifeng Sun, Zirui Zhuang, Jinming Wu, Lei Zhang, and Jianxin Liao. ChatTime: A Unified Multimodal Time Series Foundation Model Bridging Numerical and Textual Data. In *Proceedings of the AAAI Conference on Artificial Intelligence*, volume 39, pages 12694–12702, 2025.
- [55] Daoyu Wang, Mingyue Cheng, Zhiding Liu, Qi Liu, and Enhong Chen. Diffusion Auto-Regressive Transformer for Effective Self-Supervised Time Series Forecasting. *arXiv preprint arXiv:2410.05711*, 2024.
- [56] Shiyu Wang, Jiawei Li, Xiaoming Shi, Zhou Ye, Baichuan Mo, Wenze Lin, Shengtong Ju, Zhixuan Chu, and Ming Jin. TimeMixer++: A General Time Series Pattern Machine for Universal Predictive Analysis. *arXiv preprint arXiv:2410.16032*, 2024.
- [57] Haixu Wu, Jiehui Xu, Jianmin Wang, and Mingsheng Long. Autoformer: Decomposition Transformers with Auto-Correlation for Long-Term Series Forecasting. In *Neural Information Processing Systems*, volume 34, pages 22419–22430, 2021.
- [58] Haixu Wu, Hang Zhou, Mingsheng Long, and Jianmin Wang. Interpretable Weather Forecasting for Worldwide Stations with a Unified Deep Model. *Nature Machine Intelligence*, 5(6):602–611, 2023.
- [59] Hao Xue and Flora D Salim. PromptCast: A New Prompt-Based Learning Paradigm for Time Series Forecasting. *IEEE Transactions on Knowledge and Data Engineering*, 36(11):6851–6864, 2023.
- [60] An Yang, Baosong Yang, Beichen Zhang, Binyuan Hui, Bo Zheng, Bowen Yu, Chengyuan Li, Dayiheng Liu, Fei Huang, Haoran Wei, et al. Qwen2.5 Technical Report. *arXiv preprint arXiv:2412.15115*, 2024.
- [61] Silin Yang, Dong Wang, Haoqi Zheng, and Ruochun Jin. TimeRAG: Boosting LLM Time Series Forecasting via Retrieval-Augmented Generation. In *ICASSP 2025-2025 IEEE International Conference on Acoustics, Speech and Signal Processing (ICASSP)*, pages 1–5. IEEE, 2025.
- [62] Xinli Yu, Zheng Chen, Yuan Ling, Shujing Dong, Zongyi Liu, and Yanbin Lu. Temporal Data Meets LLM—Explainable Financial Time Series Forecasting. *arXiv preprint arXiv:2306.11025*, 2023.
- [63] Xinyu Yuan and Yan Qiao. Diffusion-TS: Interpretable Diffusion for General Time Series Generation. *arXiv preprint arXiv:2403.01742*, 2024.
- [64] Ailing Zeng, Muxi Chen, Lei Zhang, and Qiang Xu. Are Transformers Effective for Time Series Forecasting? In *AAAI Conference on Artificial Intelligence*, volume 37, pages 11121–11128, 2023.
- [65] Chaolv Zeng, Yuan Tian, Guanjie Zheng, and Yunjun Gao. How much can time-related features enhance time series forecasting? *arXiv preprint arXiv:2412.01557*, 2024.

- [66] Gang Zhang, Dazhi Yang, George Galanis, and Emmanouil Androulakis. Solar Forecasting With Hourly Updated Numerical Weather Prediction. *Renewable and Sustainable Energy Reviews*, 154:111768, 2022.
- [67] Wenqing Zhang, Junming Huang, Ruotong Wang, Changsong Wei, Wenqian Huang, and Yuxin Qiao. Integration of Mamba and Transformer-MAT for Long-Short Range Time Series Forecasting With Application to Weather Dynamics. In *2024 International Conference on Electrical, Communication and Computer Engineering (ICECCE)*, pages 1–6. IEEE, 2024.
- [68] Yunhao Zhang and Junchi Yan. Crossformer: Transformer Utilizing Cross-Dimension Dependency for Multivariate Time Series Forecasting. In *The Eleventh International Conference on Learning Representations*, 2023.
- [69] Haoyi Zhou, Shanghang Zhang, Jieqi Peng, Shuai Zhang, Jianxin Li, Hui Xiong, and Wancai Zhang. Informer: Beyond Efficient Transformer for Long Sequence Time-Series Forecasting. In *AAAI Conference on Artificial Intelligence*, volume 35, pages 11106–11115, 2021.
- [70] Tian Zhou, Ziqing Ma, Qingsong Wen, Liang Sun, Tao Yao, Wotao Yin, Rong Jin, et al. FiLM: Frequency Improved Legendre Memory Model for Long-Term Time Series Forecasting. In *Neural Information Processing Systems*, volume 35, pages 12677–12690, 2022.
- [71] Tian Zhou, Ziqing Ma, Qingsong Wen, Xue Wang, Liang Sun, and Rong Jin. FEDformer: Frequency Enhanced Decomposed Transformer for Long-Term Series Forecasting. In *International Conference on Machine Learning*, pages 27268–27286. PMLR, 2022.
- [72] Tian Zhou, Peisong Niu, Liang Sun, Rong Jin, et al. One Fits All: Power General Time Series Analysis by Pretrained LM. *Advances in Neural Information Processing Systems*, 36:43322–43355, 2023.
- [73] Xin Zhou, Weiqing Wang, Shilin Qu, Zhiqiang Zhang, and Christoph Bergmeir. Unveiling the Potential of Text in High-Dimensional Time Series Forecasting. *arXiv preprint arXiv:2501.07048*, 2025.
- [74] Zihao Zhou and Rose Yu. Can LLMs Understand Time Series Anomalies? *arXiv preprint arXiv:2410.05440*, 2024.

A Timestamp Encoding

The dataset utilized in this study incorporates three sampling frequencies: daily, weekly, and monthly. In the case of the daily dataset, it is represented by three-dimensional features: [DayOfWeek, DayOfMonth, DayOfYear]. For the weekly dataset, two-dimensional features are employed: [DayOfMonth, WeekOfYear]. As for the monthly dataset, the feature of [MonthOfYear] is utilized. The different time encoding calculation formulas are as follows:

$$\begin{aligned}
 \text{DayOfWeek} &= \frac{i_d}{6} - 0.5 \\
 \text{DayOfMonth} &= \frac{i_d - 1}{30} - 0.5 \\
 \text{DayOfYear} &= \frac{i_d - 1}{365} - 0.5 \\
 \text{WeekOfYear} &= \frac{i_w - 1}{52} - 0.5 \\
 \text{MonthOfYear} &= \frac{i_m}{11} - 0.5,
 \end{aligned} \tag{17}$$

where i_d , i_w , and i_m represent the daily, weekly, and monthly indexes, respectively.

B Text Input Design

In our experiment, we collect reports of all dates within the historical period to compile a text document that represents textual data describing the time series. Below, we present our text input template (the placeholders are marked by angle brackets) and an example of it.

Template

Below is historical reporting information over the past **<history_length>** **<sampling_period>**s concerning the **<target_variable>**. Based on these reports, predict the potential trends and anomalies of the **<target_variable>** for the next **<prediction_length>** **<sampling_period>**s. **<start_date1>** to **<end_date1>**: **<report1>**. **<start_date2>** to **<end_date2>**: **<report2>** ...

Example

Below is historical reporting information over the past **14 days** concerning the **stock price**. Based on these reports, predict the potential trends and anomalies of the stock price for the next **7 days**. **2025-04-01 to 2025-04-07**: Company A's shares rose steadily due to strong quarterly earnings. **2025-04-08 to 2025-04-14**: Market volatility increased amid macroeconomic uncertainty. ...

C Diffusion Step Encoding

For the m -th data point in the historical window, we use a 128-dimensional temporal embedding:

$$s_{\text{embedding}}(m) = \left(\sin\left(m/\tau^{0/64}\right), \dots, \sin\left(m/\tau^{63/64}\right), \cos\left(m/\tau^{0/64}\right), \dots, \cos\left(m/\tau^{63/64}\right) \right) \tag{18}$$

where $\tau = 10000$. Note that although our proposed model already includes global temporal information provided by timestamps, we still retain the use of temporal embedding introduced by Tashiro et al. (2021) [50] because it focuses more on time encoding starting from the historical window.

Table 4: Hyperparameters of MCD-TSF

	Monthly	Weekly	Daily
Attention heads	8	8	8
Timestamp features dim.	1	2	3
diffusion step embeddings dim.	128	128	128

Table 5: The results of models with different orders to incorporate timestamps and text information into the time series representations through TAA and TTF.

	Agr		Ene		Eco		Tra	
	MSE	MAE	MSE	MAE	MSE	MAE	MSE	MAE
TTF-TAA	0.247	0.328	0.215	0.354	0.282	0.383	0.102	0.175
TAA-TTF	0.222	0.322	0.153	0.293	0.249	0.374	0.093	0.159

D Evaluation Metrics

We compute the MSE and MAE by

$$\begin{aligned}
 MAE &= \text{mean} \left(\left| \hat{\mathcal{Y}} - \mathcal{Y}^* \right| \right) \\
 MSE &= \sqrt{\text{mean} \left(\left| \hat{\mathcal{Y}} - \mathcal{Y}^* \right|^2 \right)}.
 \end{aligned}
 \tag{19}$$

where $\hat{\mathcal{Y}}$ and \mathcal{Y}^* stand for the model predictions and the gold standard, respectively.

E Hyperparameters of MCD-TSF

As illustrated in Appendix A, the dimension of timestamp features is related to their recording frequency, with a daily frequency having a dimension of 3, a weekly frequency having a dimension of 2, and a monthly frequency having a dimension of 1. Besides, the dimension of diffusion step embeddings is 128 and the number of attention heads is 8. Table 4 summarizes these hyperparameters.

F Supplementary Results

F.1 Module Order Comparison

In experiments, we conduct a comparative analysis to investigate the impact of sequential arrangements between the TAA module and TTF module on model performance in multimodal fusion. The results are reported in Table 5, where our approach (TAA-TTF) that firstly fuses the timestamp to the time series and then integrates the text into the time series achieves better performance than the TTF-TAA model that performs the fusion operations in the reverse order.

F.2 Results of Different Horizons Setting

In Table ?? and Table 7, we present the full performance comparison (i.e., MSE and MAE on the eight domains) between the MCD-TSF model and existing studies with varying prediction horizons, whose settings are specified in Section 4.3.

F.3 Effect of the Timestamp Weight

Figure 6 presents the results of our approach on *climate*, *energy*, *environment*, and *health* domains when configured with various values of the timestamp weights, where a similar trend to the one in Section 5.2 is observed.

Table 6: Comparative MSE results between our approach and baseline models in all horizons.

(a) MSE Results 1

	Agriculture			Climate			Economy			Energy		
	6	12	18	12	24	48	6	12	18	12	24	48
Reformer	1.694	2.695	2.295	1.236	1.305	<u>1.461</u>	0.638	0.792	0.986	0.426	0.468	0.580
Autoformer	0.318	0.484	0.710	1.266	1.902	2.676	0.267	0.300	0.348	0.402	0.403	0.438
FEDformer	0.431	0.631	0.747	1.762	2.365	3.062	0.250	0.303	0.317	0.317	0.406	0.509
PatchTST	0.158	0.400	0.598	0.568	1.174	2.998	0.224	0.282	0.373	<u>0.093</u>	0.202	0.365
HCAN	0.363	0.549	<u>0.467</u>	0.887	<u>1.129</u>	1.742	0.328	0.367	0.443	0.115	<u>0.162</u>	1.115
FiLM	0.432	0.556	1.038	2.360	2.548	3.276	0.356	0.386	0.570	0.286	0.354	0.422
DLinear	0.985	1.015	2.745	0.841	0.887	1.124	0.816	1.252	1.766	0.244	0.299	0.392
TimeMixer++	0.151	0.354	0.502	0.635	1.088	2.418	0.181	0.216	0.594	0.088	0.220	0.379
Timemachine	0.140	<u>0.285</u>	0.486	0.831	1.515	3.046	<u>0.182</u>	0.273	0.389	0.122	0.295	0.376
CSDI	1.995	2.159	2.136	0.762	1.311	1.721	0.970	1.590	1.918	0.191	0.491	0.547
D3VAE	0.097	1.143	2.259	0.718	1.124	1.819	0.464	0.628	0.891	0.181	0.240	0.439
FPT	0.299	0.450	0.596	0.631	1.840	2.853	0.267	0.312	<u>0.331</u>	0.123	0.234	0.344
TimeLLM	0.312	0.480	0.483	0.830	1.270	2.151	0.219	0.258	0.350	0.103	0.197	<u>0.309</u>
MM-TSF	1.333	1.395	1.415	<u>0.592</u>	1.285	1.959	0.839	0.965	1.505	0.317	0.569	0.944
GLAFF	0.389	0.433	0.474	1.684	1.934	2.446	0.197	0.490	0.486	0.098	0.191	0.362
TimeLinear	0.410	0.528	0.554	1.059	1.662	2.447	0.258	0.303	0.421	0.175	0.247	0.361
MCD-TSF	<u>0.110</u>	0.219	0.337	0.864	1.749	2.136	0.186	<u>0.245</u>	0.317	0.088	0.153	0.219

(b) MSE Results 2

	Environment			Health			Social Good			Traffic		
	48	96	192	12	24	48	6	12	18	6	12	18
Reformer	0.308	0.316	0.336	1.555	1.798	1.839	1.287	1.443	1.502	0.267	0.343	0.429
Autoformer	0.341	0.391	0.401	1.331	1.458	<u>1.513</u>	0.940	1.452	1.469	0.141	0.159	0.178
FEDformer	0.300	0.305	0.306	1.326	1.607	1.861	1.257	1.593	1.729	0.146	0.165	0.167
PatchTST	0.251	0.254	0.257	1.316	1.598	1.753	0.825	1.141	1.234	0.108	0.128	0.138
HCAN	0.263	0.292	0.307	1.419	2.075	2.156	0.797	1.006	1.310	0.212	0.218	0.331
FiLM	0.304	0.282	<u>0.269</u>	2.062	1.716	2.249	1.510	2.136	1.834	0.136	0.162	0.178
DLinear	0.265	0.289	0.297	1.312	1.566	1.784	1.239	1.439	1.568	0.167	0.330	0.348
TimeMixer++	0.294	0.279	0.297	1.392	1.729	2.477	0.925	1.102	1.492	0.086	<u>0.100</u>	0.116
Timemachine	<u>0.257</u>	0.288	0.282	1.367	1.581	2.050	1.012	1.478	1.532	<u>0.094</u>	0.101	<u>0.110</u>
CSDI	0.277	0.310	0.287	1.309	1.813	1.933	0.828	1.149	1.359	0.113	0.115	0.119
D3VAE	0.344	0.443	0.486	2.230	1.742	1.473	0.936	1.155	1.204	0.213	0.228	0.255
FPT	0.276	0.285	0.287	1.432	1.499	1.722	<u>0.805</u>	<u>0.992</u>	1.343	0.175	0.184	0.188
TimeLLM	0.269	<u>0.275</u>	0.287	1.502	1.171	1.884	0.952	1.118	1.395	0.150	0.137	0.139
MM-TSF	0.320	0.332	0.356	<u>1.096</u>	<u>1.438</u>	1.570	0.827	1.166	<u>1.189</u>	0.205	0.227	0.243
GLAFF	0.269	0.282	0.298	1.196	1.658	1.836	0.790	1.142	1.184	0.104	0.111	0.120
TimeLinear	0.279	0.284	0.288	1.373	1.518	1.777	1.310	1.513	1.730	0.150	0.163	0.176
MCD-TSF	0.258	0.276	0.290	1.026	1.566	1.895	0.814	0.950	1.342	0.085	0.097	0.098

F.4 Effect of the Unconditional Training Probability

Figure 7 presents the results of our model with different values of the unconditional training probability p_{uncond} in various domains, namely, *agriculture*, *climate*, *economy*, *energy*, *social good*, and *traffic*. The trend is similar to the observations in Section 5.3.

Table 7: Comparative MAE results between our approach and baseline models in all horizons.

(a) MAE Results 1

	Agriculture			Climate			Economy			Energy		
	6	12	18	12	24	48	6	12	18	12	24	48
Reformer	0.933	1.209	1.309	0.927	0.964	<u>1.023</u>	0.662	0.734	0.840	0.491	0.533	0.611
Autoformer	0.428	0.538	0.648	0.892	1.075	1.343	0.414	0.438	0.467	0.471	0.479	0.501
FEDformer	0.533	0.631	0.706	1.114	1.290	1.514	0.439	0.438	0.395	0.438	0.481	0.527
PatchTST	0.258	0.426	0.528	0.594	<u>0.817</u>	1.475	0.379	0.419	0.458	0.225	0.336	0.477
HCAN	0.511	0.529	0.615	0.782	0.892	1.192	0.423	0.462	0.510	0.235	0.287	0.835
FiLM	0.471	0.559	0.702	1.224	1.243	1.639	0.479	0.509	0.632	0.425	0.451	0.499
DLinear	0.697	1.015	1.279	0.728	0.818	0.842	0.752	0.922	1.123	0.368	0.407	0.463
TimeMixer++	0.268	0.430	0.501	<u>0.617</u>	0.791	1.318	0.335	0.366	0.589	0.214	0.342	0.456
Timemachine	0.249	<u>0.345</u>	<u>0.479</u>	0.713	0.924	1.501	0.328	0.412	0.483	0.261	0.395	0.463
CSDI	1.005	1.063	1.077	0.682	0.836	1.138	0.787	1.015	1.104	0.306	0.525	0.586
D3VAE	0.669	0.727	1.071	0.680	0.825	1.177	0.543	0.620	0.674	0.329	0.380	0.547
FPT	0.416	0.517	0.597	0.621	1.117	1.433	0.412	0.448	0.451	0.252	0.384	0.450
TimeLLM	0.426	0.524	0.528	0.712	0.864	1.187	0.362	0.389	0.440	0.242	0.344	<u>0.422</u>
MM-TSF	0.711	0.798	0.825	0.608	0.892	1.239	0.736	0.805	0.921	0.406	0.575	0.787
GLAFF	0.518	0.549	0.591	1.080	1.178	1.367	0.344	0.579	0.573	0.223	0.313	0.443
TimeLinear	0.459	0.530	0.657	0.811	1.008	1.283	0.403	0.440	0.527	0.321	0.381	0.466
MCD-TSF	<u>0.251</u>	0.323	0.392	0.763	1.015	1.134	<u>0.333</u>	<u>0.380</u>	<u>0.409</u>	<u>0.220</u>	<u>0.292</u>	0.367

(b) MAE Results 2

	Environment			Health			Social Good			Traffic		
	48	96	192	12	24	48	6	12	18	6	12	18
Reformer	0.435	0.449	0.461	0.853	0.862	0.866	0.760	0.879	0.906	0.439	0.494	0.566
Autoformer	0.415	0.443	0.456	0.859	0.860	0.888	0.586	0.753	0.836	0.255	0.271	0.285
FEDformer	0.392	0.419	0.425	0.874	0.948	1.007	0.797	0.953	1.028	0.283	0.296	0.298
PatchTST	<u>0.362</u>	0.368	0.371	0.786	0.868	0.937	0.445	0.570	0.714	0.201	0.235	0.253
HCAN	0.387	0.428	0.445	0.783	0.910	0.913	0.459	0.602	0.701	0.241	0.333	0.631
FiLM	0.352	0.377	0.436	1.013	1.198	1.219	0.931	1.016	1.193	0.263	0.272	0.341
DLinear	0.380	0.379	0.387	0.804	0.881	0.950	0.769	0.851	0.924	0.303	0.435	0.465
TimeMixer++	0.441	0.445	0.458	0.771	0.900	1.127	<u>0.430</u>	0.564	0.773	<u>0.149</u>	0.170	<u>0.188</u>
Timemachine	0.370	0.384	0.388	0.777	0.846	1.012	0.494	0.570	0.755	0.161	<u>0.172</u>	<u>0.188</u>
CSDI	0.378	0.389	0.406	0.735	0.890	0.948	0.487	0.594	0.648	0.232	0.241	0.243
D3VAE	0.472	0.558	0.577	0.868	0.946	<u>0.867</u>	0.550	0.658	<u>0.689</u>	0.355	0.374	0.378
FPT	0.397	0.383	0.437	0.797	0.866	0.868	0.450	<u>0.561</u>	0.749	0.310	0.318	0.324
TimeLLM	0.445	<u>0.370</u>	<u>0.380</u>	<u>0.704</u>	<u>0.787</u>	0.964	0.554	0.628	0.712	0.224	0.227	0.234
MM-TSF	0.450	0.463	0.488	0.706	0.767	0.809	0.484	0.620	0.692	0.382	0.409	0.417
GLAFF	0.378	0.380	0.438	0.750	0.875	0.918	0.429	0.586	0.714	0.198	0.203	0.217
TimeLinear	0.377	0.388	0.397	0.799	0.847	0.906	0.777	0.880	0.994	0.275	0.307	0.318
MCD-TSF	0.369	0.384	0.385	0.651	0.871	0.912	0.440	0.531	0.736	0.138	0.164	0.174

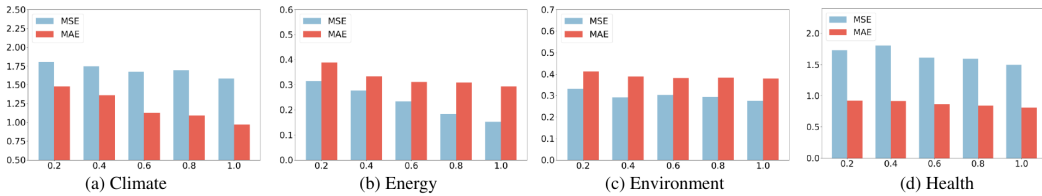


Figure 6: Results of our approach on different domains when configured with various values of the timestamp weights (i.e., the $\lambda = 0.2, 0.4, 0.6, 0.8, 1.0$).

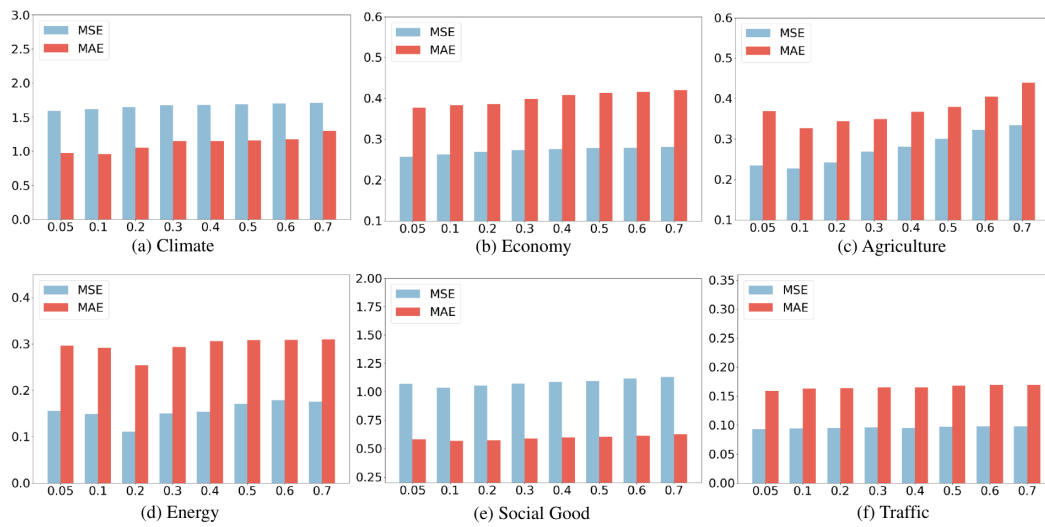


Figure 7: The model performance with changes in the unconditional training probability.